

FULL PAPER**Supplementary Material***(Received 00 Month 20XX; accepted 00 Month 20XX)***1. Dataset**

We recorded a dataset [1] in a network of underground pedestrian streets in Umeda, the main commercial and business district of Osaka, which is the second largest metropolitan area of Japan. The entire complex connects four train stations and several department stores and shopping centers and is visited by about 2.5 million people everyday.

We carried out our experiments on a weekday between 10 AM and 4 PM at an intersection of two particular streets of this underground network, to which we refer to as *the environment* henceforth¹ (see Figure 1). Since the experiment was performed on a weekday, students and colleagues commuting together with their friends constitute a considerable portion of the crowd. Therefore, the dataset contains an abundant number of social groups, among which social interaction takes place at varying levels.



Figure 1. Experiment environment. The people marked with yellow move as a group and interact. Two of the laser range finders are shown in red.

Two sorts of data are collected in the experiment; (i) range data and (ii) video data². These data are utilized in the following manner:

- Range data are incorporated with the particle filter based tracking algorithm of [2] for obtain-

¹The environment contains one main street, which intersects with a smaller street almost perpendicularly (see Figure 1). The main street is 59.5 m long and 6.6 m wide and the small street 18 m long and 3.6 m wide.

²The range data are obtained using 16 laser range finders equipped with Hokuyo UTM-30LX positioned along the walls (shown on Figure 1 in red). The video data are recorded by two camcorders, where one camera is positioned at each end of the main street.

ing the pedestrian trajectories. By these means, a total of 12791 people are tracked during the 6-hour experiment and the normalized density map illustrated in Figure 2 is obtained³.

- The video data are used to establish the ground truth regarding group motion and interaction relation. By positioning two camcorders at each end of the street, we get a good sight of the pedestrians walking in both directions as seen in the sample video frame shown in Figure 1.

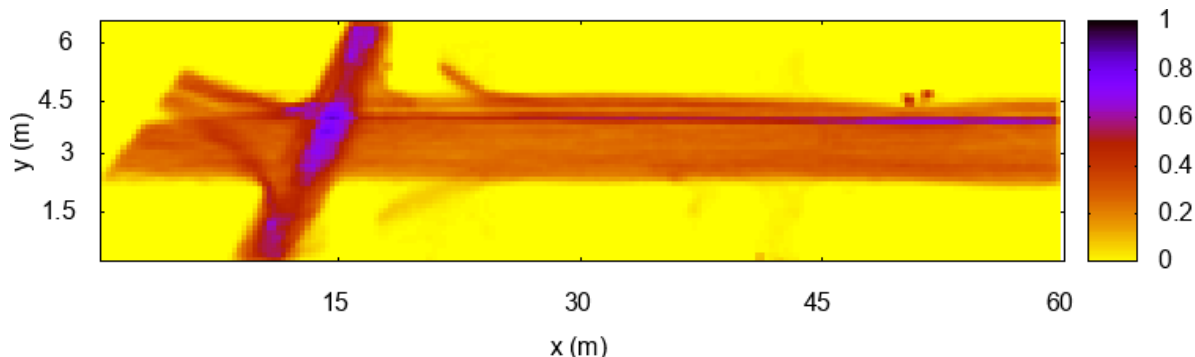


Figure 2. Normalized density map of the environment.

After examining the data closely, we decided to focus on 2-people (2p) and 3-people (3p) groups and the solitary individuals, i.e. non-groups. The reasons for this choice are the following:

- (1) Groups of 4p, 5p, 6p do not usually move in an abreast formation and break into subgroups of 2p or 3p, making them the basic building blocks of all groups [3].
- (2) The number of observations of 2p and 3p groups are enough to characterize their behavior, whereas larger groups are observed seldom⁴.

2. Ground truth

Video data are used for establishing the ground truth regarding the following:

- Group relation: The possible states regarding this relation are “group” or “non-group”. We term any two pedestrians who are observed simultaneously in the environment a *pair* and let the coders label the pairs which constitute a group. The complementary case of non-group is automatically attributed to all remaining pairs.
- Interaction relation: Those pairs, which are labeled as “group” in the previous step, are examined and one of the four possible labels for intensity of interaction \mathcal{I} is assigned to each pair. The possible labels are 0, 1, 2, and 3, where $\mathcal{I} = 0$ indicates no-interaction, $\mathcal{I} = 1$ indicates weak interaction, $\mathcal{I} = 2$ indicates mild interaction and $\mathcal{I} = 3$ indicates intense interaction. In the remaining of the paper, we will often use the shortening \mathcal{I}_i for $\mathcal{I} = i$.

2.1. Method of annotation

In order to assess errors due to coding fatigue and coder’s bias, each relation (group/non-group and intensity) is labeled by two different coders.

In the first stage of the coding (i.e. identification of the pedestrian groups), the coders watch the walking patterns, age, gender, or clothing, and define which pedestrians constitute a group [4].

³The higher density lane along the main street is due to the Braille blocks.

⁴We have 22 4p groups, 2 5p groups, 3 6p groups and 1 7p group.

In the second stage (assessing intensity of interaction), we consider only the pedestrians which are labeled to be a member of a social group at the first stage. This reduces the amount of data that each coder has to view and thus provides a more efficient coding.

At this stage, the coders are asked to label the pedestrian groups with respect to their intensity of interaction by selecting one of the four options of 0, 1, 2, 3. Clearly, this is a highly subjective measure. In order not to bias the coders' assessment, we only defined the resolution (i.e. the number of interaction levels as 4) but we did not give any guidelines on what can be considered as weak, mild or strong in terms of interaction intensity. Instead, we let the coders grasp a feeling about different levels of interaction intensity through a free-viewing task. In other words, for understanding the variations on interaction intensity, we let the coders initially watch for 3 hours the videos of the pedestrians which are labeled to be in a group relation at the previous stage.⁵

2.2. Inter-coder reliability

For evaluating the consistency of the two annotations, we use inter-rater reliability measures of Cohen's κ coefficient⁶ [5, 6], and Krippendorff's α for ordinal data [7, 8] (see Table 1).

Table 1. Inter-rater reliability measures of Cohen's κ and Krippendorff's α for group relation and intensity of interaction, respectively. Cohen's κ is corrected for prevalence.

Annotation	Statistics	Value
Group relation	Cohen's κ	0.96
Interaction intensity	Krippendorff's α	0.67

For interpreting Cohen's κ values, we use the guidelines of Fleiss et al. [9], who consider $\kappa < 0.4$ as poor, 0.40 to 0.75 as fair to good, and over 0.75 as excellent agreement. Thus, the consistency in labeling group relation is regarded to be almost perfect based on these principles. Here we also note that it is common in the literature to rely on much lower values of $\kappa \approx 0.5$ [10–12].

For interpreting the level of agreement in labeling intensity of interaction, we use the policy of Krippendorff [7]. Krippendorff points out to the difficulty of establishing universal reliability bands and states that 0.67 has been adopted as cut-off value for better or worse. Since our values are around this widely accepted boundary, we consider the inter-rater agreement to be fairly good.

2.3. Distribution of labels

Having confirmed that the coders have consistent labels, in the rest of the analysis, we pick the annotations of one of the coders randomly and base our ground truth on her labels. According to the annotations of the randomly picked coder, we have the number of pedestrians, pairs and groups as given in Table 2.

As for group relation, there are 634 2p groups, 75 3p groups and 10892 non-groups (i.e. pedestrians who are not in any group). The second column of Table 2-(a) denotes the pairs relating 2p, 3p groups and non-groups. The number of pairs in 2p and 3p groups are straightforward to compute from the number of groups. However, for non-group pairs, we consider the pedestrians who satisfy the following two conditions: (i) observations overlapping in time for at least 5 seconds, (ii) being at least once at a distance of 3 meters or less⁷. In this way, we eliminate the non-group pairs who are clearly not in group relation and consider only those which have a possibility of being in a group.

⁵Here, we note that the total duration of the trajectories of 2p and 3p groups is less than 6 hours and thus a 3-hour free viewing task corresponds to watching approximately half of the groups, which is considered sufficient to get an idea of variation of intensity patterns.

⁶with prevalence correction

⁷Distances of more than 3 meters are extremely improbable in interacting groups, [1]

Moreover, for the 2p and 3p groups, the distribution of interacting pairs at various intensities are given in Table 2-(b).

Table 2. (a) The number of 2p, 3p groups and pedestrians who are not in any group (non-groups). (b) The number of pedestrians interacting with varying intensities.

	(a)		(b)			
	N	N_{pair}	Intensity			
2p	634	634	0	1	2	3
3p	75	225	66	97	386	85
Non-groups	10892	34243	57	65	90	13

3. Motion models

This section presents details on the definition of the variables used in modeling of joint motion, the preprocessing of trajectory points, analysis of variance of empirical distributions and expands the description of corresponding motion model of each variable.

3.1. Definition of joint motion attributes

Figure 3 illustrates an example of a 3p group composed of pedestrians p_i , p_j and p_k . We define our variables on this sample 3p group, but they are defined in an analogous way for 2p groups as well.

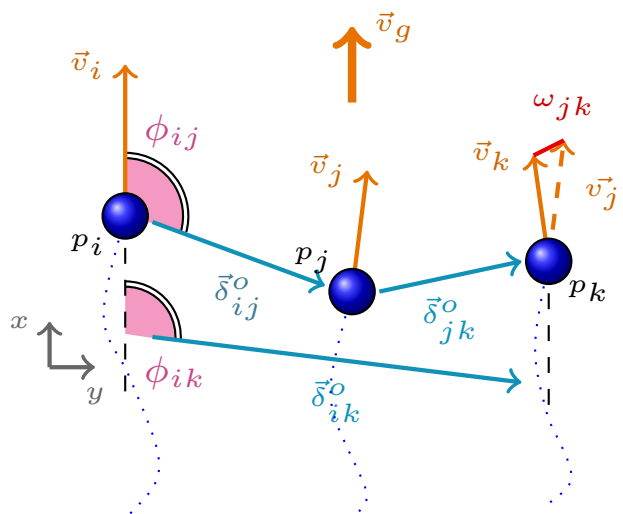


Figure 3. Parameters used in modeling joint motion illustrated on a 3p group.

In examining the joint behavior, we focus particularly on three joint motion attributes, namely (i) *interpersonal distance* δ (ii) *relative orientation* ϕ with respect to motion direction and (iii) *absolute difference of velocity vectors* ω .

- (1) Although we will focus on the attribute δ , i.e. the absolute value of the distance between pedestrians in a pair, in the development of some of our models it will be useful to take in consideration the components of the displacement vector $\vec{\delta}$, and in order to eliminate the effects of changing motion direction due to taking curves or avoiding behavior, such components are better defined in relation to the group motion direction.

The interpersonal distance of p_i with respect to his peer p_j , is denoted with $\vec{\delta}_{ij}$. Its explicit components are computed projecting the displacement vector on group motion direction, \hat{v}_g , which is the unit vector along the mean velocity of the group:

$$\vec{v}_g = \frac{\sum_{i=0}^N \vec{v}_i}{N}.$$

Projecting the displacement vector from p_i to p_j , i.e. $\vec{\delta}_{ij}$ on \hat{v}_g , the x -component δ_x of interpersonal distance δ_{ij} is found to be (see Figure 3) as follows,

$$\delta_x = \vec{\delta}_{ij} \cdot \hat{v}_g.$$

Similarly, the y -component δ_y is obtained by a projection onto a unit vector orthogonal to \hat{v}_g (obtained through a $\pi/2$ clockwise rotation). The interpersonal distance relation of a pair $\{p_i, p_j\}$ is then given by distance of each pedestrian to their peers, expressed in the projection coordinate frame introduced above, namely by the set of vectors $\{\vec{\delta}_{ij}, \vec{\delta}_{ji} = -\vec{\delta}_{ij}\}$.

- (2) The relative orientation ϕ_{ij} , of p_j with respect to the motion direction of p_i , is defined as the angle between the velocity vector of p_i and the displacement vector from p_i to p_j , i.e. $\frac{\vec{v}_i \cdot \vec{\delta}_{ij}}{|\vec{v}_i| |\delta_{ij}|}$. To represent relative orientation of a pair $\{p_i, p_j\}$, we use the pair $\{\phi_{ij}, \phi_{ji}\}$ ⁸.
- (3) The third joint motion attribute of the pair $\{p_i, p_j\}$, namely their absolute difference of velocity vectors ω_{ij} , is simply defined as the magnitude of the difference vector

$$\omega_{ij} = |\vec{v}_i - \vec{v}_j|.$$

Figure 3 demonstrates the absolute difference of velocity for the pair $\{p_j, p_k\}$, ω_{jk} .

3.2. Preprocessing

The trajectories are obtained by processing the raw range data. Subsequently, they are first exposed to several preprocessing operations and then tested against several criteria, where only those trajectories which satisfy these criteria are used in the analysis.

The preprocessing of the trajectories is composed of a smoothing operation of the data points to obtain samples at uniform time intervals. The reason for this is that the range sensors return readings in an irregular manner in time and at a very high frequency, which makes some samples redundant.⁹

To obtain readings over uniform time intervals, we average the values falling in the same 100 msec time window as follows:

$$\vec{x}(t_0) = (x_{t_0}, y_{t_0}) = \{(\bar{x}_t, \bar{y}_t) \mid t_0 - 0.1 \leq t < t_0\}.$$

and then compute the velocity as

$$\vec{v}(t_0) = (\vec{x}(t_0 + 0.1) - \vec{x}(t_0 - 0.1))/0.2$$

The joint motion attributes of interpersonal distance δ , relative orientation ϕ and absolute difference of velocities ω are derived from the trajectory points exposed to the smoothing operation described

⁸Each angle is defined using the individual velocity \vec{v}_{ij} . Nevertheless, when the pedestrians are part of a group and moving together, we may expect to have $\vec{v}_{ij} \approx \vec{v}_{ji}$ and thus $\phi_{ij} \approx \phi_{ji} + \pi$.

⁹This sampling is particularly useful in the computation of pedestrian velocity, since it provides a smoother trajectory and thus a more reliable and stable velocity.

above.

Subsequently, we test the trajectories against several conditions. The first condition relates the continuity of locomotion. Namely, we focus on the behavior of the pedestrians during their active motion and skip the parts where they keep still (to wait, meet, greet etc). Therefore, we set a velocity threshold at 0.5 m/sec and consider the data points where the pedestrians are moving at a higher velocity than this threshold value¹⁰.

The second condition concerns the length of the trajectory. Specifically, we consider trajectories which are sufficiently long, in order to comment on group relation or interaction in a plausible way. We set the threshold value for trajectory length to 10 meters and omit the pedestrians who cover a shorter distance (for instance, by only taking a curve from the small street to the main street, see Figure 2).

The third condition, which applies only to 3p groups, relates degree of neighborhood. Since pedestrians in 3p groups may switch their position resulting in varying degrees of neighborhood, which affects distance relation drastically, we exclude the 3p groups that are subject to position switches and consider the ones which keep a stable neighborhood structure.

3.3. Analysis of variance of empirical distributions

We confirm the qualitative observations of Section 4 in the Main Text through a quantitative way using analysis of variance as illustrated in Table 3¹¹. As expected, in detection of group relation all three attributes have quite small p-values.

Furthermore, also in detection of intensity of interaction in 2p groups, the p-values suggest a statistically significant difference for all three joint motion attributes δ , ϕ and ω .

Finally, based on the p-values for 3p groups, we may notice that ω appears to be the best indicator in distinction of intensity of interaction, whereas δ achieves low scores even though the curves in Figure 4 in the Main Text suggest otherwise, particularly for second neighbors. This is probably due to the fact that the number of samples at each intensity level is not well-balanced as shown in Table 2.

Table 3. Analysis of variance for empirical distributions. The joint motion attributes, which are considered to serve useful in distinction of group relation and intensity of interaction are illustrated in bold face.

	δ	ϕ	ω
Group relation	$< 10^{-4}$	$< 10^{-4}$	$< 10^{-4}$
Intensity relation in 2p	$< 10^{-4}$	$< 10^{-4}$	$< 10^{-4}$
Intensity relation in 3p	0.60 and 0.42	0.95	0.03

3.4. Modelling interpersonal distance

Since interpersonal distance depends to a great extent on the degree of neighborhood, we treat 2p groups and the first neighbors in 3p groups in the same manner, whereas second neighbors in 3p groups and non-groups are handled in different ways.

3.4.1. Interpersonal distance for groups

The work of [1] introduces a potential that describes the position dynamics of two pedestrians in a socially interacting group. Such a *discomfort potential*, i.e. the function that pedestrians try to

¹⁰For a justification of this value, refer to [13].

¹¹For the ϕ attribute, we use in the Anova only the values $\phi \in [0, \pi/2]$ to be able to highlight differences in spread between distributions with the same average value $\approx \pi/2$.

minimize in order to maximize their comfort in social interaction, depends on the sum of two terms, one of them being the distance between pedestrians δ and the other one the relative orientation ϕ ¹². Using methods from statistical physics, [1] shows that δ and ϕ result to be statistically independent variables, and in particular they show that the probability distribution for δ is given by

$$p(\delta|\beta, r_0) = \delta \exp\left(\frac{-\beta(\delta - r_0)^2}{\delta r_0}\right). \quad (1)$$

Here the parameter r_0 is the preferred distance for social interaction, while β is, in the statistical physics terminology, the *inverse temperature* (namely, the larger β is the more the pedestrian system will be ordered and the distribution narrowly centered on r_0).

According to [1], the interaction of first neighbors in a 3p group is given by the same potential, and thus, ignoring second order terms, their distance distribution will be given by the same model used in the 2p situation. For second neighbors, they do not provide a closed form for the probability distribution of distance, since the non-trivial structure (V shaped formation) of the group allows only for a numerical solution. Nevertheless, if the angle in the V formation is assumed to be close to 180 degrees, namely if the pedestrians are assumed to walk abreast (which results to be a good approximation in most cases, as discussed also by Moussaïd et al., [14]), the distance between second neighbors can be modeled as the convolution of the unimodal model with itself. This multi-modal framework is expressed as follows:

$$p(\delta|\beta, r_0) = (p * p)\left(\delta \exp\left(\frac{-\beta(\delta - r_0)^2}{\delta r_0}\right)\right). \quad (2)$$

3.4.2. Interpersonal distance for non-groups

Proximity models for pedestrians who are not engaged in social interaction usually refer to the guidelines defined by Hall (see Figure 4-(a)). Although these may make sense for standing pedestrians, they do not apply to actively moving pedestrians, in particular when there is a prominent flow direction along a street as in our case. Figure 4 contrasts the definitions of Hall with the empirical distribution of distances between non-groups in our dataset. This proves that simple ring like structures do not suffice to model the actual behavior of mobile non-groups.

Examining Figure 4-(b) closely, we may conclude that when the environment presents a prominent flow direction, there is an area, on the front and back of the pedestrian (i.e., along the y direction, according to our previous definition), and with a width comparable to body size, in which the probability of finding another pedestrian is extremely low. As a simplified, but nevertheless quite effective, model, we may assume (recalling that we are considering only pedestrians with a distance $\delta \leq R$, with $R = 3$ meters) that the variables δ_x and δ_y have uniform distributions subject to the conditions $\delta = \sqrt{\delta_x^2 + \delta_y^2} \leq R$ and $\delta_x \geq r$, where r is the “human body size” (Hall’s intimate distance, for which we assume the value $r=0.5$ meters). Geometrically, this means that the relative pedestrian distance will be uniformly distributed inside two circular segments, located symmetrically with respect to the y axis and at an r distance between them, and thus the probability of finding the pedestrians at a distance $r \leq \delta \leq R$ is proportional to $\delta \arccos(r/\delta)$. Through an elementary integration, the normalized formula for the explicit probability distribution function results to be¹³

¹²Such angle is actually defined in a slightly different way by [1], namely with respect to the group goal direction (empirically assumed to be aligned to the group velocity).

¹³On the other hand in an isotropic environment we could assume uniform distribution between r and R and, by trivial

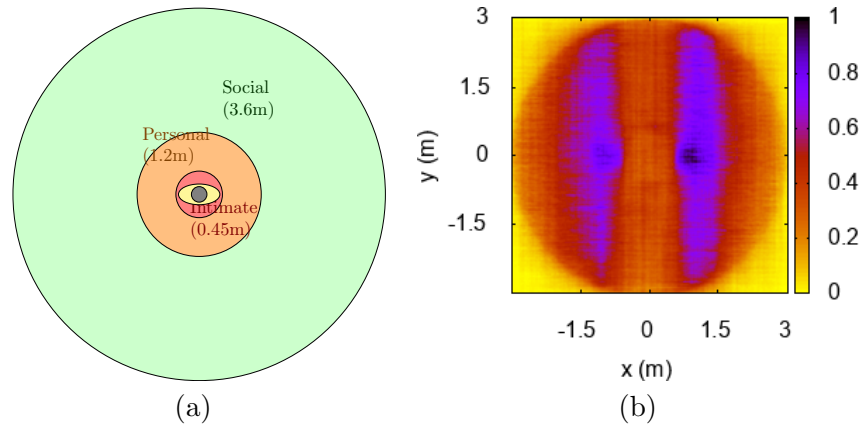


Figure 4. (a) Hall's definitions for proxemics. (b) Empirical distribution of interpersonal distance on cumulative data for non-groups.

$$p(\delta|R, r) = \frac{4}{\pi R^2 - 2R^2 \arcsin\left(\frac{r}{R}\right) - 2r\sqrt{R^2 - r^2}} \delta \arccos\left(\frac{r}{\delta}\right). \quad (3)$$

3.5. Modelling relative orientation

For ϕ , the analytical model of [1] leads to a Gaussian distribution. Their model presents nevertheless, for reasons of analytical tractability, a cuspidal point in the potential at $\phi = 0, \pi$, which is the reason they obtain a Gaussian distribution instead of a *von Mises*¹⁴. Since we do not need in this work to derive the distribution from first principles, we will directly use the more appropriate *von Mises* distribution without paying regard to the groups size or the degree of neighborhood¹⁵. The model is given as follows,

$$p(\phi|\nu, \kappa) = \frac{\exp(\kappa \cos(\phi - \nu))}{2\pi I_0(\kappa)}, \quad (4)$$

where ν denotes the mean value, κ is analogous of $1/\sigma^2$ in the normal distribution, and I_0 is the modified Bessel function of the first kind with order zero [15].

Since we do not pay regard to be positioned on the right or left side with respect to motion direction, both pedestrians in a pair are treated in the same manner, which leads to a distribution with two peaks. Thus, we use a linear combination of two von Mises distributions to represent the relative orientation of a pair,

$$\Phi(\phi|\nu_{1,2}\kappa_{1,2}) = \alpha_1(\phi|\nu_1, \kappa_1) + \alpha_2(\phi|\nu_2, \kappa_2), \quad (5)$$

which, due to the obvious left-right symmetry of the problem (for every person on the right side, there has to be another person on the left), can be simplified to

$$\Phi(\phi|\nu, \kappa) = 0.5p(\phi|\nu, \kappa) + 0.5p(\phi|\nu + \pi, \kappa). \quad (6)$$

geometrical considerations, obtain $p = 2\delta/(R^2 - r^2)$.

¹⁴Note that Von Mises distribution is the generalization of a Gaussian describing a smooth circular (angle) distribution.

¹⁵Again, according to the analysis of [1], a different model for the first and second neighbor distribution should be introduced to assess the presence of a V formation. For the purpose of this work, as we did in the development of the convolution model for the second neighbor distance, we may follow [14] and assume that 3p groups walk roughly in an abreast formation.

3.6. Modelling absolute difference of velocities

Pedestrians in a group move towards the same target point independent of the groups size and neighborhood. Even though there may be slight deviations from the target direction due to various reasons such as avoidance behavior or interaction, the expected value is always around 0. Therefore, we approximate the x and y components of ω with a Gaussian with 0 mean, which makes ω come from a Rayleigh distribution,

$$p(\omega|\sigma) = \frac{\omega}{\sigma^2} \exp \frac{-\omega^2}{2\sigma^2}. \quad (7)$$

For non-groups, we may expect the distributions of the the x and y components of the velocity difference to have non-zero mean value ν , and thus it is necessary to use the corresponding generalization of the Rayleigh distribution, namely the Rice distribution

$$p(\omega|\nu, \sigma) = \frac{\omega}{\sigma^2} \exp \left(\frac{-\omega^2 - \nu^2}{2\sigma^2} \right) I_0 \left(\frac{\omega \nu}{\sigma^2} \right), \quad (8)$$

where I_0 is again the modified Bessel function of the first kind with order zero.

Furthermore, we need to distinguish the case of pedestrians moving in the same direction (for which we expect $\nu \ll v$, v being the pedestrian average velocity) and pedestrians moving in opposite directions (for which we expect $\nu \approx 2v$). The proposed model thus reads

$$p(\omega|C_{1,2}, \nu_{1,2}, \sigma_{1,2}) = \sum_{i=1,2} C_i \frac{\omega}{\sigma_i^2} \exp \left(\frac{-\omega^2 - \nu_i^2}{2\sigma_i^2} \right) I_0 \left(\frac{\omega \nu_i}{\sigma_i^2} \right). \quad (9)$$

4. Calibration of models

The observed distributions are expressed in terms of the histograms relating each set, whereas the corresponding model parameters are solved minimizing the squared error between the observations and the relating models through a golden section search.

In case the models are governed by more than a single parameter, we adopt an alternating strategy (for instance, as in Equation 1 or Equation 6). For solving these systems, we minimize the squared error in an iterative way alternating between the parameters. In other words, we first optimize for one parameter keeping the other(s) fixed and repeat this procedure for other parameters until satisfactory convergence is achieved.

In addition, we shuffle each observation set of interest and randomly select 20% of the samples and calibrate the model parameters on this subset. Repeating this procedure 50 times¹⁶, we compute the mean values and standard deviations regarding the model parameters, which gives an idea on the sensitivity (i.e. dependence) of the parameters on training set.

4.1. Sensitivity of model parameters in group identification

The models proposed in Sections 3.4, 3.5 and 3.6 are calibrated as explained in Section 4. The resulting model parameters are shown to differ between groups and non-groups in a significant way, which proves that the proposed models can be used in estimation of group relation. Moreover,

¹⁶By randomly selecting 20% of the set and repeating this process 50 times, the probability that a particular observation is not used in estimating the model parameters in any epoch, falls below 10^{-4} , which is quite small.

the parameters are shown not to be sensitive to the changes in the set of observation which is used to estimate them. This indicates that the models can stably be constructed from any subset of observations (of a reasonable size). In what follows, the details of these statements are presented.

4.1.1. Sensitivity of models of interpersonal distance regarding group relation

The dashed curves in Figure 2-(a) in the Main Text demonstrate the models constructed at a sample run. This figure proves that the models approximate the observations in a quite effective way, capturing general tendency with a good accuracy.

Table 4. Sensitivity of model parameters for δ with respect to group relation. Calibration is repeated 50 times by on a random subset of observations composed of 20% of the entire observation set.

	N_{Total}	β	r_0
2p	634	18 ± 1.7	748 ± 8
First neighbors in 3p	150	14.7 ± 0.2	788 ± 1
Second neighbors in 3p	75	10.4 ± 0.3	716 ± 3

In addition, Table 4 presents the variation on the 2p and 3p group motion models in relation to changes in the subset of observations used in estimating them^{17 18}. These values prove that the standard deviations of β and r_0 are small enough to lead to similar models when different training sets are used¹⁹.

4.1.2. Sensitivity of models of relative orientation

In Figure 2-(b) in the Main Text, we illustrate the relative orientation models for 2p, 3p groups and non-groups with dashed lines. This figure ascertains that the three empirical distributions as well as the models differ significantly between groups and non-groups, which is already determined quantitatively by the p-values presented in Table 3.

Table 5. Sensitivity of model parameters for ϕ with respect to group relation. Calibration is repeated 50 times on a different randomly chosen subset of observations composed of 20% of the entire observation set.

	N_{Total}	ν	κ
2p	634	1.56 ± 0.002	7.06 ± 0.62
3p	225	1.57 ± 0.01	2.53 ± 0.81
Non-groups	10892	0.15 ± 0.02	5.31 ± 0.93

Besides, the variation on the relative orientation model parameters given in Table 5 prove that the dependence of the parameters on the chosen subset of observations is quite limited, suggesting the estimation process to be quite robust. In addition, it ascertains that the variation on the parameters is considerably smaller than the variation between different (competing) categories (i.e. groups vs non-groups).

4.1.3. Sensitivity of models of absolute difference of velocities

Figure 2-(c) in the Main Text shows the three models (in dashed lines) for absolute difference of velocities for 2p, 3p groups and non-groups. These models approximate the observations in an

¹⁷Note that the interpersonal distance relating non-groups does not involve any parameters.

¹⁸The lower value assumed by r_0 for 3p groups is consistent with the fact that pedestrians are actually not abreast but in a V formation, and thus the distance of second neighbors is smaller than twice the distance of first neighbors.

¹⁹In particular, we may notice that standard deviations are small with respect to both the absolute values of parameters and to the difference between the values that such parameters assume in different categories.

accurate manner and in a good agreement with the analysis of Table 3. They are also distinct enough to serve useful in identification of group relation.

Table 6. Sensitivity of model parameters for ω with respect to group relation. Calibration is repeated 50 times on a different randomly chosen subset of observations composed of 20% of the entire observation set.

	N_{Total}	σ	
2p	634	0.23 ± 0.004	
3p	225	0.24 ± 0.008	
	N_{Total}	$\nu_{1,2}$	$\sigma_{1,2}$
Non-groups	10892	0.30 ± 0.01	0.28 ± 0.01
		2.40 ± 0.01	0.48 ± 0.009

Moreover, Table 6 demonstrates that the sensitivity of the model parameters to changes in calibration subsets is limited.

4.2. Sensitivity of model parameters in estimation of intensity of interaction

We present the sensitivity of the model parameters relating each level of intensity of interaction using different calibration subsets, similar to Section 4.1.

4.2.1. Sensitivity of models of interpersonal distance

The parameters of interpersonal distance models presented in Tables 7 and 8 are in agreement with our hypothesis described in the Main Text. Nevertheless, the variation of parameters are comparable (although always smaller) to the differences that such parameters assume between neighboring categories, namely between \mathcal{I}_i and \mathcal{I}_{i+1} . This is not completely surprising, given the arbitrary and subjective nature of these labels. Nevertheless, the difference between the two extremes, \mathcal{I}_0 and \mathcal{I}_3 , is much larger than the parameter variation

Table 7. Model parameters of [1] for δ in 2p groups with varying intensity of interaction. Calibration is repeated 50 times on a different randomly chosen subset of observations composed of 20% of the entire observation set.

Intensity	N_{Total}	β	r_0
0	66	10.14 ± 3.33	863.74 ± 37.28
1	97	14.22 ± 3.31	791.56 ± 28.50
2	386	21.65 ± 2.17	749.17 ± 7.96
3	85	26.21 ± 3.80	723.56 ± 14.08

Table 8. Model parameters of [1] for δ in 3p groups with varying intensity of interaction. At every calibration round, 20% of the total number of relating samples is used.

Intensity	First neighbors			Second neighbors		
	N_{3p}^1	β	r_0	N_{3p}^2	β	r_0
0	10	14.2 ± 8.9	851 ± 139	9	21.2 ± 8.1	750 ± 63
1	23	15.2 ± 5.9	828 ± 57	10	17.8 ± 9.5	718 ± 74
2	36	25.2 ± 4.9	767 ± 18	15	15.2 ± 10.2	691 ± 109
3	3	28.4 ± 1.6	791 ± 118	2	22.8 ± 3.4	658 ± 19

4.2.2. Sensitivity of models of relative orientation

The evolution of the parameters in Table 9 with increasing intensity of interaction supports the hypotheses presented in Section 1 of the Main Text. Moreover, the standard deviation values are

quite smaller than the separation of the means for 2p groups (at least when the extremes are compared), which proves not only the distinction of the models but also the resilience of the calibration against varying parameter estimation subsets. However, for 3p groups although the expected evolution in κ is observed through $\mathcal{I} = 0$ to $\mathcal{I} = 2$, the patterns is broken for $\mathcal{I} = 3$ probably due to small number of samples (5).

Table 9. Model parameters for ϕ with varying intensity of interaction. Von Mises model is used for all pairs. At every calibration round, 20% of the total number of relating samples is used.

Intensity	2p groups			3p groups		
	N_{2p}	μ	κ	N_{3p}	μ	κ
0	66	1.53 ± 0.01	3.24 ± 1.42	19	1.71 ± 0.76	1.04 ± 0.91
1	97	1.56 ± 0.007	5.85 ± 1.81	33	1.61 ± 0.20	1.85 ± 1.29
2	386	1.56 ± 0.002	7.63 ± 0.70	51	1.56 ± 0.01	4.47 ± 1.85
3	85	1.56 ± 0.003	8.86 ± 2.68	5	1.92 ± 0.60	2.65 ± 1.94

4.2.3. Sensitivity of models of absolute difference of velocities

The effect of interaction is grasped by the proposed models since the σ values get smaller with increasing intensity of interaction as seen in Table 10. In addition, the variation on the calibrated parameters with shuffling and random selection, suggests that the distinction is significant for both 2p and 3p groups. Nevertheless, as stated also for the other variables, the variances in parameters are comparable to the differences in the same parameters between neighboring categories, suggesting again the use of the extremes \mathcal{I}_0 and \mathcal{I}_3 as benchmarks for intensity estimation.

Table 10. Rayleigh model parameters for ω with varying intensity of interaction.

Intensity	2p groups		3p groups	
	N_{Tot}	σ	N_{Tot}	σ
0	66	0.28 ± 0.01	19	0.26 ± 0.01
1	97	0.25 ± 0.01	33	0.25 ± 0.01
2	386	0.23 ± 0.005	51	0.23 ± 0.009
3	85	0.21 ± 0.008	5	0.21 ± 0.02

5. Observations on model parameters in estimation of intensity of interaction

As briefly explained in Section 1 in the Main Text, our hypothesis is that when two people interact, a more regular pattern is observed in their joint behavior. In other words, non-interacting pedestrians have a larger flexibility on their motion patterns, whereas interacting peers have (i) a stable and short distance, (ii) an abreast formation, and (iii) a smaller difference between velocities. In addition, for increasing intensities of interaction, we expect to see a shift towards a more regular behavior in terms of all joint motion attributes.

Therefore, for increasing intensities of interaction we expect to observe the following:

- (1) Interpersonal distance δ should decrease with increasing intensity, which defines a smaller preferred distance between peers (namely, we expect r_0 to decrease with intensity). Moreover, its variation should drop pointing to a more steady group structure (β increasing with density).
- (2) Relative orientation ϕ must be distributed around $\pm\pi/2$ for all cases but with decreasing dispersion (increasing κ), suggesting a more abreast formation.
- (3) Absolute difference of velocities ω should decrease and adopt a more compact distribution (decreasing σ) as intensity of interaction grows.

In what follows, we discuss on agreement of the empirical observations with the above listed statements. Moreover, for each case, we demonstrate the concerning models and comment on their accuracy in modeling the distinctive characteristics.

5.1. Observations on models of interpersonal distance

Figure 3-(a) in the Main Text presents the empirical distributions of δ regarding 2p groups with varying intensities of interaction. Our hypothesis implies that as intensity of interaction grows, peers keep a stable and reasonably close distance throughout their interaction, which leads $\bar{\delta}$ to be distributed around a shorter preferred distance with a smaller deviation, as clearly supported by these empirical distributions. Also note that the p-value for analysis of variance of these four distributions is found to be smaller than 10^{-4} , which ascertains that the difference between these distributions is statistically significant.

In addition, the models given in dashed lines follow the actual distributions to a considerable degree. Moreover, parameters of these models presented in Table 7 are in agreement with our hypothesis. In explicit terms, with growing intensity, β increases pointing out to the increasing concentration of the distribution, whereas r_0 decreases showing a smaller preferred distance between peers. In addition, the variation on the parameters are concluded to be insignificant in comparison to their mean values.

Figures 4-(a) and (b) in the Main Text demonstrate the behavior of δ for first and second neighbors, respectively, in 3p groups for varying intensities of interaction. As seen in Figure 4-(a) in the Main Text, δ has a peak around a smaller value and with a smaller variation with increasing intensity of interaction from 0 to 3, as expected. However, only for $\mathcal{I} = 3$ the variation is larger than expected, which is probably due to the fact that the number of observations are not distributed in a balanced manner and the samples from second neighbors with $\mathcal{I} = 3$ are quite smaller than the others. This phenomenon is observed in terms of model parameters as well (see Table 8).

Figure 4-(b) in the Main Text demonstrates that δ does not present any distinction from $\mathcal{I} = 0$ to $\mathcal{I} = 2$ but for $\mathcal{I} = 3$ it is distributed around smaller values in a more concentrated way. These observation are confirmed by the calibrated parameters as well. In other words, while the expected values of β do not seem to present any distinction, r_0 decreases with increasing intensity, but the deviation on the estimated variables are quite high. Therefore, a similar conclusion is drawn also for second neighbors, that more samples are necessary to build stable models.

5.2. Observations on models of relative orientation

Figure 3-(b) in the Main Text presents the empirical distribution of ϕ regarding 2p groups for varying intensities of interaction. As suggested by our hypothesis, the motion of pedestrians become more abreast with growing intensity of interaction and the decreasing dispersion of the curves in Figure 3-(b) in the Main Text support this statement.

In addition, this tendency is captured in terms of the model parameters as well. As expected, the mean values are around $\pi/2$ for all cases. Nevertheless, the increasing values of κ in Table 9 indicate that the distributions adopt a more concentrated pattern as intensity increases, proving that the proposed models reflect the tendency in an efficient manner.

Figure 4-(c) in the Main Text presents the relative orientation pattern for 3p groups. From these curves we conclude that ϕ for 3p groups presents a similar pattern to that of 2p groups but the distinction is not as clear as in dyads. However, this pattern is broken for $\mathcal{I} = 3$, probably due to insufficient number of samples.

This can be observed in terms of the κ parameter which increases from 1.04 to 4.47 as in Table 9. Nevertheless, comparing Figure 4-(c) and Figure 3-(b) in the Main Text, and the κ parameters in right and left columns of Table 9, one may conclude that the distinction between different patterns

of ϕ with varying levels of intensity are not as profound as the one for 2p groups.

5.3. *Observations on models of absolute difference of velocities*

Figure 3-(c) and Figure 4-(d) in the Main Text present the empirical distributions and concerning models for ω of 2p and 3p groups, respectively, with varying intensity of interaction. As expected, the peak of the absolute difference of velocities get smaller and the distribution less sparse with increasing intensities of 2p and 3p groups, the former being more prominent.

In addition, the effect of interaction is grasped by the proposed models since the σ values get smaller with increasing intensity of interaction as seen in Table 9. In addition, the variation on the calibrated parameters with shuffling and random selection, suggests that the distinction is significant for both 2p and 3p groups.

References

- [1] Zanlungo F, Ikeda T, Kanda T. Potential for the dynamics of pedestrians in a socially interacting group. *Physical Review E*. 2014;89:012811.
- [2] Glas D, Miyashita T, Ishiguro H, et al. Laser-based tracking of human position and orientation using parametric shape modeling. *Advanced robotics*. 2009;23:405–428.
- [3] Zanlungo F, Kanda T. Do walking pedestrians stably interact inside a large group? analysis of group and sub-group spatial structure. In: *CogSci*; 2013.
- [4] McPhail C, Wohlstein R. Using film to analyze pedestrian behavior. *Sociological Methods and Research*. 1982;10:347.
- [5] Cohen J. Weighted kappa: Nominal scale agreement provision for scaled disagreement or partial credit. *Psychological bulletin*. 1968;70:213.
- [6] Di Eugenio B, Glass M. The kappa statistic: A second look. *Computational linguistics*. 2004;30:95–101.
- [7] Krippendorff K. Reliability in content analysis. *Human communication research*. 2004;30:411–33.
- [8] Hayes AF, Krippendorff K. Answering the call for a standard reliability measure for coding data. *Communication methods and measures*. 2007;1:77–89.
- [9] Fleiss JL, Levin B, Paik MC. *Statistical methods for rates and proportions*. John Wiley & Sons; 2013.
- [10] Obrist M, Seah SA, Subramanian S. Talking about tactile experiences. In: *ACM CHI*. ACM; 2013. p. 1659–1668.
- [11] Germesin S, Wilson T. Agreement detection in multiparty conversation. In: *ICMI 2009*. ACM; 2009. p. 7–14.
- [12] Byrt T. How good is that agreement? *Epidemiology*. 1996;7:561.
- [13] Zanlungo F, Chigodo Y, Ikeda T, et al. Experimental study and modelling of pedestrian space occupation and motion pattern in a real world environment. In: *Pedestrian and evacuation dynamics 2012*. Springer International Publishing; 2014. p. 289–304.
- [14] Moussaïd M, Perozo N, Garnier S, et al. The walking behaviour of pedestrian social groups and its impact on crowd dynamics. *PLoS ONE*. 2010;5:e10047.
- [15] Mardia KV, Jupp PE. *Directional statistics*. John Wiley & Sons Inc; 2000.